Hindawi Publishing Corporation
Discrete Dynamics in Nature and Society
Volume 2012, Article ID 814069, 13 pages
doi:10.1155/2012/814069

Research Article

Pattern Formation in a Cross-Diffusive Ratio-Dependent Predator-Prey Model

Xinze Lian,[1] Yanhong Yue,[2] and Hailing Wang[3]

[1] *Chengdu Institute of Computer Application, Chinese Academy of Sciences, Chengdu 610041, China*
[2] *School of Foreign Language, Wenzhou University, Wenzhou 325000, China*
[3] *College of Mathematics and Physics, Chongqing University of Posts and Telecommunications, Chongqing 400065, China*

Correspondence should be addressed to Xinze Lian, xinzelian@163.com

Received 29 September 2012; Accepted 3 November 2012

Academic Editor: Yonghui Xia

This paper presents a theoretical analysis of evolutionary process that involves organisms distribution and their interaction of spatial distribution of the species with self- and cross-diffusion in a Holling-III ratio-dependent predator-prey model. The diffusion instability of the positive equilibrium of the model with Neumann boundary conditions is discussed. Furthermore, we present novel numerical evidence of time evolution of patterns controlled by self- and cross-diffusion in the model and find that the model dynamics exhibits a cross-diffusion controlled formation growth to spots, stripes, and spiral wave pattern replication, which show that reaction-diffusion model is useful to reveal the spatial predation dynamics in the real world.

1. Introduction

Pattern formation is a topic in mathematical biology that studies how structures and patterns in nature evolve over time [1–12]. One of the mainstream topics in pattern formation involves the reaction-diffusion mechanisms of two chemicals, originally proposed by Turing [13] in 1952. In 1972, Segel and Jackson [14] called attention to the Turing's ideas that would be also applicable in population dynamics. At the same time, Gierer and Meinhardt [15] gave a biologically justified formulation of a Turing model and studied its properties by numerical simulations. Levin and Segel [11] suggested that the scenario of spatial pattern formation is a possible origin of planktonic patchiness. A significant amount of work has been done using this idea in the field of mathematical biology by Cantrell and Cosner [2], Hoyle [5], Murray [8], Okubo and Levin [16], and others [17–19].

In recent years, many scientists have paid considerable attention to diffusive ratio-dependent predator-prey models, especially those with Holling III functional response

[20–23]. In [23], the author studied the spatial pattern formation of the following ratio-dependent predator-prey model:

$$\begin{aligned}\frac{\partial u}{\partial t} &= ru\left(1-\frac{u}{K}\right)-\frac{au^2v}{u^2+m^2v^2}+D_{11}\nabla^2u,\\ \frac{\partial v}{\partial t} &= \frac{bvu^2}{u^2+m^2v^2}-dv+D_{22}\nabla^2v,\end{aligned} \tag{1.1}$$

where u and v are prey and predator density, respectively. r represents the intrinsic growth rate of the prey, K is the carrying capacity of the prey in the absence of predator, a is the maximum consumption, b is the conversion efficiency of food into offspring, m is the predator interference parameter, and d is the per capita predator death rate. $\nabla^2 = \partial^2/\partial x^2 + \partial^2/\partial y^2$ is the usual Laplacian operator in two-dimensional space. D_{11} and D_{22} are the self-diffusion coefficients that imply the movement of individuals from a higher to lower concentration region. In addition, the author showed that spots and stripes-spots patterns could be observed in pure Turing instability, and spiral pattern emerged in Hopf and Turing instability [23].

On the other hand, the predator-prey system models such a phenomenon: pursuit-evasion-predators pursuing prey and prey escaping the predators [18, 19, 24, 25]. In other words, in nature, there is a tendency that the preys would keep away from predators and the escape velocity of the preys may be taken as proportional to the dispersive velocity of the predators. In the same manner, there is a tendency that the predators would get closer to the preys, and the chase velocity of predators may be considered to be proportional to the dispersive velocity of the preys. Keeping these in view, cross-diffusion arises, which was proposed first by Kerner [26] and first applied in competitive population system by Shigesada et al. [27].

There has been a considerable interest in investigating the stability behavior of a predator-prey system by taking into account the effect of self- and cross-diffusion [17, 18, 28–35]. Cross-diffusion expresses the population fluxes of one species due to the presence of the other species. However, in the studies on spatiotemporal dynamics of the ratio-dependent predator-prey system with functional response, little attention has been paid to study on the effect of cross-diffusion.

In this paper, we mainly focus on the spatiotemporal dynamics of a cross-diffusion ratio-dependent predator-prey model with Holling III functional response. In the next section, we establish the cross-diffusion model and derive the sufficient conditions for Turing instability. Then, we present and discuss the results of pattern formation via numerical simulation in Section 3. Finally, some conclusions are drawn.

2. The Model and Analysis

2.1. The Model

We firstly pay attention to the spatially extended ratio-dependent predator-prey model with self- and cross-diffusion, which is as follows:

$$\begin{aligned}\frac{\partial u}{\partial t} &= ru\left(1-\frac{u}{K}\right)-\frac{au^2v}{u^2+m^2v^2}+D_{11}\nabla^2u+D_{12}\nabla^2v,\\ \frac{\partial v}{\partial t} &= \frac{bvu^2}{u^2+m^2v^2}-dv+D_{21}\nabla^2u+D_{22}\nabla^2v,\end{aligned} \tag{2.1}$$

where D_{12} and D_{21} are cross-diffusion coefficients that express population fluxes of the preys and predators resulting from the presence of the other species, respectively.

We consider the model on a square domain Ω. We also add to the reaction-diffusion equation model positive initial conditions:

$$u(x,y,0) > 0, \qquad v(x,y,0) > 0 \quad (x,y) \in \Omega = (0,L) \times (0,L). \tag{2.2}$$

It is natural to assume that nothing enters this model and nothing exits this model. Thus, we will take zero-flux boundary conditions for the flat domain:

$$\left.\frac{\partial u}{\partial \nu}\right|_{\partial\Omega} = \left.\frac{\partial v}{\partial \nu}\right|_{\partial\Omega} = 0. \tag{2.3}$$

In the above, L denotes the size of the system in square domain, and ν is the outward unit normal vector of the boundary $\partial\Omega$.

For simplicity, we nondimensionalize model (2.1) with the following scaling:

$$u \longrightarrow \frac{u}{K}, \qquad v \longrightarrow \frac{mv}{K}, \qquad t \longrightarrow rt. \tag{2.4}$$

Then model (2.1) can be rewritten as

$$\begin{aligned} \frac{\partial u}{\partial t} &= u(1-u) - \frac{\alpha u^2 v}{u^2 + P^2} + d_{11}\nabla^2 u + d_{12}\nabla^2 v, \\ \frac{\partial v}{\partial t} &= \frac{\beta u^2 v}{u^2 + v^2} - \gamma v + d_{21}\nabla^2 u + d_{22}\nabla^2 v, \end{aligned} \tag{2.5}$$

where $\alpha = a/rm$, $\beta = b/r$, $\gamma = d/r$, $d_{11} = D_{11}/r$, $d_{12} = D_{12}/rm$, $d_{21} = D_{21}m/r$, $d_{22} = D_{22}/r$. In addition, we call

$$D = \begin{pmatrix} d_{11} & d_{12} \\ d_{21} & d_{22} \end{pmatrix} \tag{2.6}$$

the diffusive matrix.

2.2. Summary of the Noncross Diffusion Model

We first consider the case of spatially homogeneous solutions. In this case spatial model (2.5) is equivalent to the ordinary differential equation model

$$\begin{aligned} \frac{du}{dt} &= u(1-u) - \frac{\alpha u^2 v}{u^2 + v^2} \triangleq f(u,v), \\ \frac{dv}{dt} &= \frac{\beta u^2 v}{u^2 + v^2} - \gamma v \triangleq g(u,v). \end{aligned} \tag{2.7}$$

It can be seen that model (2.7) has two nonnegative real equilibria as follows.

(i) The equilibrium point $E = (1, 0)$ corresponding to extinction of the predator is a saddle point.

(ii) The equilibrium point $E^* = (u^*, v^*)$ which is corresponding to a nontrivial stationary state coexistence of prey and predator, where

$$u^* = \frac{\beta - \sqrt{\alpha^2\beta\gamma - \alpha^2\gamma^2}}{\beta}, \qquad v^* = \frac{\sqrt{\alpha^2\beta\gamma - \alpha^2\gamma^2}N^*}{\alpha\gamma}. \tag{2.8}$$

It is easy to see that $u^* > 0$ and $v^* > 0$ when $\beta - \gamma > 0$ and $\beta - \sqrt{\alpha^2\beta\gamma - \alpha^2\gamma^2} > 0$ hold.

Besides, Turing instability at the coexistence equilibrium E^* of the model (2.5) has been analysis without cross-diffusion. Here, we only give a summary [23]. The characteristic equation at the steady state E^* of model (2.5) without cross-diffusion is

$$|J_k - \lambda I| = 0, \tag{2.9}$$

where, $J_k = J - \mathrm{diag}(d_1, d_2)k^2$, and J is given by

$$J = \begin{pmatrix} \dfrac{\partial f}{\partial u} & \dfrac{\partial f}{\partial v} \\ \dfrac{\partial g}{\partial u} & \dfrac{\partial g}{\partial v} \end{pmatrix}_{E^*} \triangleq \begin{pmatrix} f_u & f_v \\ g_u & g_v \end{pmatrix} = \begin{pmatrix} \dfrac{-\beta^2 + 2\sqrt{-\alpha^2\gamma^2(\gamma-\beta)}}{\beta^2} & -\dfrac{\alpha\gamma(2\gamma-\beta)}{\beta^2} \\ -2\dfrac{(\gamma-\beta)\sqrt{-\alpha^2\gamma(\gamma-\beta)}}{\alpha\beta} & 2\dfrac{\gamma(\gamma-\beta)}{\beta} \end{pmatrix}, \tag{2.10}$$

and the trace and determinant of matrix J is as follows:

$$\begin{aligned} \mathrm{tr}(J) &= f_u + f_v, \\ \det(J) &= f_u g_v - f_v g_u. \end{aligned} \tag{2.11}$$

Now (2.9) can be solved, yielding the so-called characteristic polynomial of the original model (2.5) without cross-diffusion:

$$\lambda^2 - \mathrm{tr}(J_k)\lambda + \det(J_k) = 0, \tag{2.12}$$

where

$$\begin{aligned} \mathrm{tr}(J_k) &= \mathrm{tr}(J) - (d_1 + d_2)k^2, \\ \det(J_k) &= d_1 d_2 k^4 - \left(d_2 f_u + d_1 g_v\right)k^2 + \det(J). \end{aligned} \tag{2.13}$$

The roots of (2.12) yield the dispersion relation:

$$\lambda_{1,2}(J_k) = \frac{1}{2}\left(\operatorname{tr}(J_k) \pm \sqrt{\operatorname{tr}(J_k)^2 - 4\det(J_k)}\right). \tag{2.14}$$

And an equilibrium is Turing instability means that it is an asymptotically stable equilibrium of nonspatial model (e.g., model (2.7)) but is unstable with respect to solutions of spatial model (e.g., model (2.5)). One can know that the stability of nonspatial model is guaranteed if the following conditions hold

$$\operatorname{tr}(J) = f_u + g_v < 0, \tag{2.15}$$

$$\det(J) = f_u g_v - f_v g_u > 0. \tag{2.16}$$

Then, the Turing instability sets in when at least one of (2.15) or (2.16) the following conditions is violated. However, it is evident that the first condition $\operatorname{tr}(J_k) < 0$ is not violated when the condition $f_u + g_v < 0$ is met. Hence, only the violation of condition $\det(J_k) > 0$ gives rise to diffusion-driven instability. Thus, the condition for Turing instability is given by

$$\det(J_k) = d_1 d_2 k^4 - f_u d_2 k^2 - d_1 g_v k^2 + f_u g_v - f_v g_u < 0. \tag{2.17}$$

In summary, a general linear analysis shows that the necessary conditions for yielding Turing patterns are given by

$$\begin{aligned} f_u + g_v &< 0, \\ f_u g_v - f_v g_u &> 0, \end{aligned} \tag{2.18}$$

$$\begin{aligned} d_2 f_u + d_1 g_v &> 0, \\ \left(d_2 f_u + d_1 g_v\right)^2 &> 4 d_1 d_2 \left(f_u g_v - f_v g_u\right). \end{aligned} \tag{2.19}$$

In fact, condition (2.18) enssured, by the definition that the equilibrium (u^*, v^*) is stable for model (2.5) without diffusion model (2.7). (u^*, v^*) becomes unstable for model (2.5) with diffusion if $\operatorname{Re}(\lambda_{1,2}(J_k))$ bifurcate from negative value to positif one. From (2.17), simple algebraic computations lead to (2.19).

2.3. Dynamic Analysis of the Spatial Model

To study the effect of cross-diffusion on the model system, set $u = u^* + \tilde{u}$, $v = v^* + \tilde{v}(|\tilde{u}|, |\tilde{v}| \ll 1)$, we consider the linearized $(\tilde{u}, \tilde{v})$ form of system as follows:

$$\begin{aligned} \frac{\partial \tilde{u}}{\partial t} &= f_u \tilde{u} + f_v \tilde{v} + d_{11}\nabla^2 \tilde{u} + d_{12}\nabla^2 \tilde{v}, \\ \frac{\partial \tilde{v}}{\partial t} &= g_u \tilde{u} + g_v \tilde{v} + d_{21}\nabla^2 \tilde{u} + d_{22}\nabla^2 \tilde{v}. \end{aligned} \tag{2.20}$$

Following [18], the characteristic equation of the linearized system is given by

$$\lambda^2 - \operatorname{tr}\left(\widetilde{J}_k\right)\lambda + \det\left(\widetilde{J}_k\right) = 0, \tag{2.21}$$

where $\widetilde{J}_k = J - Dk^2$, and

$$\begin{aligned} \operatorname{tr}\left(\widetilde{J}_k\right) &= \operatorname{tr}(J) - k^2 \operatorname{tr}(D), \\ \det\left(\widetilde{J}_k\right) &= \det(D)k^4 - \left(d_{11}g_v - d_{12}g_u - d_{21}f_v + d_{22}f_u\right)k^2 + \det(J). \end{aligned} \tag{2.22}$$

The Turing instability sets in when at least one of the following conditions is violated:

$$\operatorname{tr}\left(\widetilde{J}_k\right) < 0, \qquad \det\left(\widetilde{J}_k\right) > 0. \tag{2.23}$$

The first condition $\operatorname{tr}(\widetilde{J}_k) = \operatorname{tr}(J_k)$, which is evident that $\operatorname{tr}(J_k)$ is not violated when the condition $\operatorname{tr}(J) = f_u + g_v < 0$ is met. Hence, only the violation of condition $\det(\widetilde{J}_k) > 0$ gives rise to diffusion-driven instability. Thus, the condition for diffusion-driven instability occurs when

$$\det\left(\widetilde{J}_k\right) = \det(D)k^4 - \left(d_{11}g_v - d_{12}g_u - d_{21}f_v + d_{22}f_u\right)k^2 + \det(J) < 0. \tag{2.24}$$

Based on the above discussions, we can get the following theorem.

Theorem 2.1. *If the following conditions are true:*

$$\begin{aligned} f_u + g_v &< 0, \\ d_{11}g_v + d_{22}f_u &< 0, \\ d_{11}g_v - d_{12}g_u - d_{21}f_v + d_{22}f_u &> 0, \\ \left(d_{11}g_v - d_{12}g_u - d_{21}f_v + d_{22}f_u\right)^2 &> 4(d_{11}d_{12} - d_{21}d_{12})\left(f_u g_v - f_v g_u\right), \end{aligned} \tag{2.25}$$

then the positive equilibrium E^* of model (2.5) *is cross-diffusion-driven instability (i.e., Turing instability).*

Proof. In view of $f_u + g_v < 0$ and $d_{11}g_v + d_{22}f_u < 0$, it follows that

$$\operatorname{tr}\left(\widetilde{J}_k\right) < 0, \qquad \det\left(\widetilde{J}_k\right) > 0 \tag{2.26}$$

when $d_{12} = 0$ and $d_{21} = 0$. This implies the positive equilibrium E^* is asymptotic stable in the absent of cross-diffusion.

A necessary condition for cross-diffusive instability is given by

$$d_{11}g_v - d_{12}g_u - d_{21}f_v + d_{22}f_u > 0, \tag{2.27}$$

otherwise $\det(\widetilde{J}_k) > 0$ for all $k > 0$ since $\det(D) > 0$ and $\det(J) > 0$.

For the instability, we must have $\det(\widetilde{J}_k) < 0$ for some k. And we notice that $\det(\widetilde{J}_k)$ achieves its minimum:

$$\min_{\mu_i} \sigma_2 = \frac{4\det(D)\det(J) - \left(d_{11}g_v - d_{12}g_u - d_{21}f_v + d_{22}f_u\right)^2}{4\det(D)} \tag{2.28}$$

at the critical value $k_c^2 > 0$ when

$$k_c^2 = \frac{d_{11}g_v - d_{12}g_u - d_{21}f_v + d_{22}f_u}{2\det(D)}. \tag{2.29}$$

As a consequence, if $d_{11}g_v - d_{12}g_u - d_{21}f_v + d_{22}f_u > 0$ and $(d_{11}g_v - d_{12}g_u - d_{21}f_v + d_{22}f_u)^2 > 4(d_{11}d_{12} - d_{21}d_{12})(f_u g_v - f_v g_u)$ hold, then $\det(\widetilde{J}_k) < 0$ is valid. Hence E^* is an unstable equilibrium with respect to model (2.5). This finishes the proof. □

In Figure 1, based on the results of Theorem 2.1, we show the dispersal relation of r with α. The green, red, and blue curves represent Hopf, self-diffusion Turing, and self-cross-diffusion Turing bifurcation curve, respectively. They separate the parametric space into five domains. The domain below the Hopf bifurcation curve is stable, the domain above the self-diffusion Turing bifurcation curve is unstable, and the domain above self-cross-diffusion Turing bifurcation curve is unstable. Hence, among these domains, only the domain (IV) satisfies conditions of Theorem 2.1, and we call domain (IV) as Turing space, where the Turing instability occurs and the Turing patterns may be undergone.

3. Pattern Formation

In this section, we perform extensive numerical simulations of the spatially extended model (2.5) in 2-dimensional (2D) spaces, and the qualitative results are shown here. Our numerical simulations employ the nonzero initial (2.2) and zero-flux boundary conditions (2.3) with a system size of 200×200 by using a finite-difference methods. We use the standard five-point approximation for the 2D Laplacian with the zero-flux boundary conditions. And the time step and the grid width used in the simulations are $\tau = 0.01$ and $\Delta h = 0.25$, respectively. The parameters are fixed as

$$\alpha = 2.5, \qquad \beta = 1.1, \qquad \gamma = 1.05, \qquad d_{11} = 0.2, \qquad d_{22} = 0.2. \tag{3.1}$$

Initially, the entire system is placed in the steady state (u^*, v^*), and the propagation velocity of the initial perturbation is thus on the order of 5×10^{-4} space units per time unit. And the system is then integrated for 1000 000 time steps, and the last images are saved. After the initial period during which the perturbation spreads, either the system goes into a time-dependent state, or to an essentially steady state (time independent).

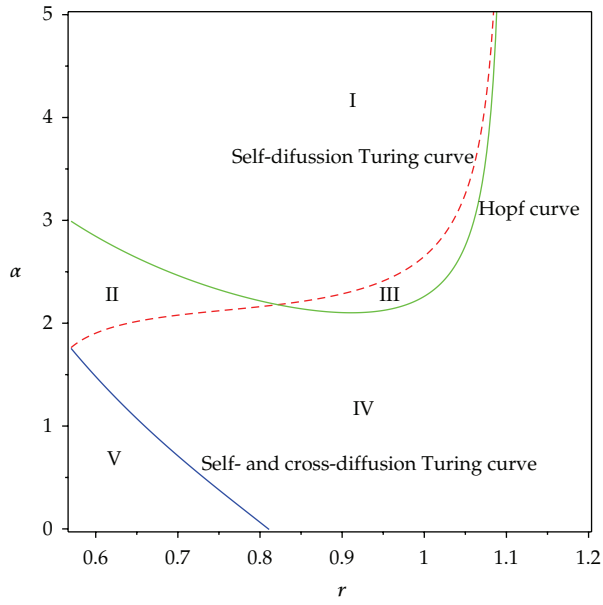

Figure 1: The dispersal relation of r with α. Parameters: $\beta = 1.3$, $d_{11} = 0.2$, $d_{12} = 0.05$, $d_{21} = 0.35$, $d_{22} = 0.2$. The green, red, and blue curves represent Hopf, self-diffusion Turing, and self-cross-diffusion Turing bifurcation curve, respectively. They separate the parametric space into five domains, and domain (IV) is called Turing space.

With parameters (3.1), the positive equilibrium of model (2.5) is $(u^*, v^*) = (0.4793, 0.1046)$. Let $d_{12} = d_{21} = 0$, that is, we first consider Turing instability in the case of self-diffusion model. It is easy to conclude that $\mathrm{tr}(J) < 0$, $\det(J) > 0$, and for all k, $\mathrm{tr}(J_k) < 0$ and $\det(J_k) > 0$. Hence, in this case, there is nonexistence of Turing instability in the self-diffusion model (2.5).

Next, we consider the effect of the cross-diffusion in model (2.5), let $d_{21} = 0.05$, $d_{12} \in (0.2, 0.8)$, and other parameters are fixed as (3.1). It is easy to know that $\mathrm{tr}(\widetilde{J}_k) < 0$ for all k, and $\det(\widetilde{J}_k) < 0$ for some k. That is to say, in this case, Turing instability can occur. And in Figure 2, we show five typical Turing pattern of prey u in model (2.5) with parameters set (3.1) and d_{12} change from 0.4 to 0.76. From Figure 2, one can see that values for the concention u are represented in a color scale varying from blue to red. And on increasing the control cross-coefficient d_{12}, the sequences "spots patterns (Figure 2(a)) $\rightarrow$ spot-strips coexist patterns (Figure 2(b)) $\rightarrow$ strip patterns (c.f., Figure 2(c)) $\rightarrow$ hole-strips coexist patterns (Figure 2(d)) $\rightarrow$ holes patterns (Figure 2(e))" can be observed.

For the sake of learning the pattern formation in model (2.5) further, in the following, we select a special perturbed initial condition for investigating the evolutionary process of the infected spatial pattern, the initial condition is introduced as

$$u(x, y, 0) = u^*,$$
$$v(x, y, 0) = \begin{cases} 0.2, & \text{if } (x - 100)^2 + (y - 200)^2 < 200, \\ 0, & \text{otherwise,} \end{cases} \tag{3.2}$$

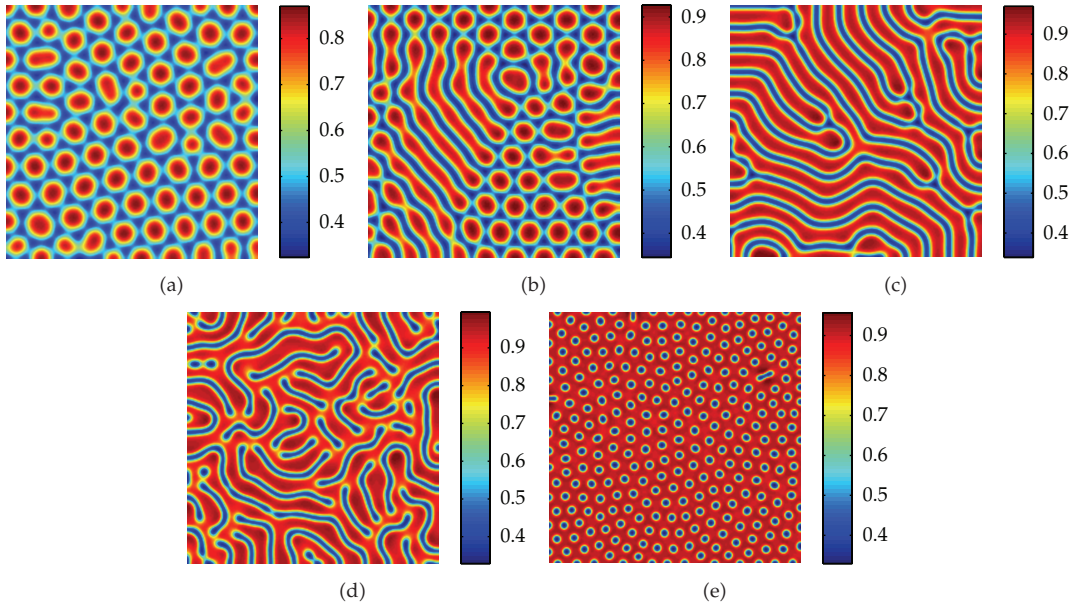

Figure 2: Patterns obtained with model (2.5) for (a) $d_{12} = 0.4$, (b) $d_{12} = 0.55$, (c) $d_{12} = 0.65$, (d) $d_{12} = 0.70$, (e) $d_{12} = 0.76$ and the other parameters are fixed as (3.1). Time: $t = 10000$.

which is a circle in (x, y) plane. The parameters are taken the same as Figure 2(a). Then, we can observe that after the decay of target patterns, the spots pattern prevails over the whole domain finally (c.f. Figure 3(d)).

Besides Turing patterns (c.f., Figures 2 and 3), there exhibits spiral wave pattern self-replication in model (2.5). As an example, in Figure 4, we show spiral patterns with $\alpha = 2.5$, $\beta = 1.3$, $\gamma = 1.1$, $d_{11} = 0.7$, $d_{12} = 0.05$, $d_{21} = 0.01$, $d_{22} = 1$. In this case, the equilibrium is $(u^*, v^*) = (0.0980, 0.0418)$. In order to make the image more clearly, the system size is 400×400 and the grid width Δh is 0.5. One can see the random initial distribution leads to the formation of macroscopic spiral patterns (c.f., Figure 4(a)). In other words, in this case, small random fluctuations will be strongly amplified by diffusion, leading to nonuniform population distributions. For the sake of learning the dynamics of this case further, we show time-series plots (c.f., Figure 4(b)). From Figure 4(b), one can see that the system gives rise to periodic oscillations in time, which is the reason why the spiral pattern emerges.

Thanks to the insightful works of Medvinsky et al. [36] and Upadhyay et al. [37], we have studied the spiral wave pattern for an initial condition discussed in the following equations. In this this case, we employ $\Delta h = 0.5$, and the system size is 400×400. The parameters set are same as Figure 4. The initial condition is given by

$$\begin{aligned} u(x, y, 0) &= u^* - \varepsilon_1 (x - 80)(x - 320), \\ v(x, y, 0) &= v^* - \varepsilon_2 (y - 100) - \varepsilon_2 (y - 300), \end{aligned} \tag{3.3}$$

where $\varepsilon_1 = 3 \times 10^{-7}$ and $\varepsilon_2 = 1 \times 10^{-4}$.

The initial conditions are deliberately chosen to be unsymmetrical in order to make any influence of the corners of the domain more visible. Snapshots of the spatial distribution

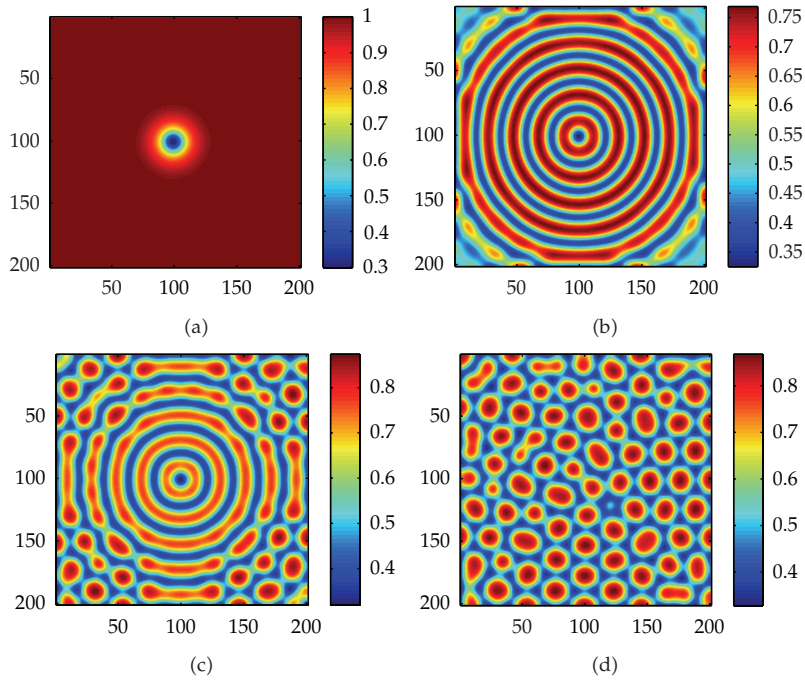

Figure 3: The process of spiral patterns of u for parameters: $\alpha = 2.2$, $\beta = 1.1$, $\gamma = 1.05$, $d_{11} = 0.2$, $d_{12} = 0.05$, $d_{21} = 0.4$, $d_{22} = 0.2$. Time: (a) $t = 50$, (b) $t = 500$, (c) $t = 1000$, (d) $t = 2000$.

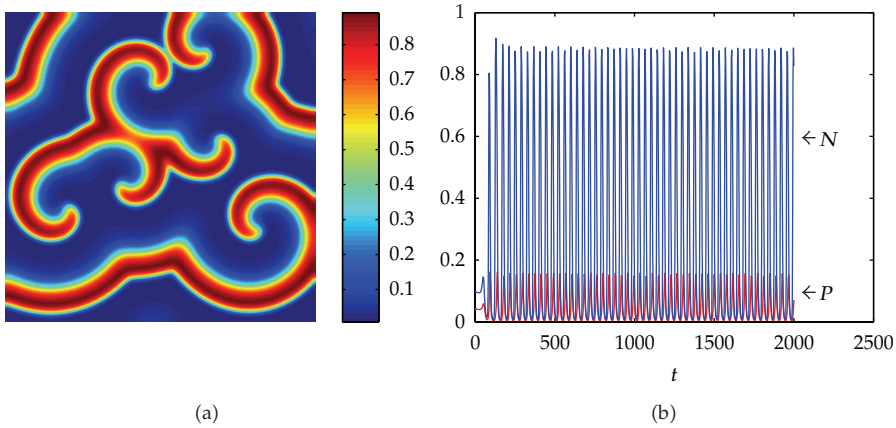

Figure 4: Dynamical behaviors of model (2.5) with the parameters: $\alpha = 2.5$, $\beta = 1.3$, $\gamma = 1.1$, $d_{11} = 0.7$, $d_{12} = 0.05$, $d_{21} = 0.01$, $d_{22} = 1$ at $t = 2000$. (a) Spiral pattern. (b) Time-series plots.

arising from (3.3) are shown in Figure 5 for $t = 0, 100, 250, 500$. Figure 5(a) shows that for the model (2.5) with initial conditions (3.3), the formation of the irregular patchy structure can be preceded by the evolution of a regular spiral spatial pattern. Note that the appearance of the spirals is not induced by the initial conditions. The center of each spiral is situated in a

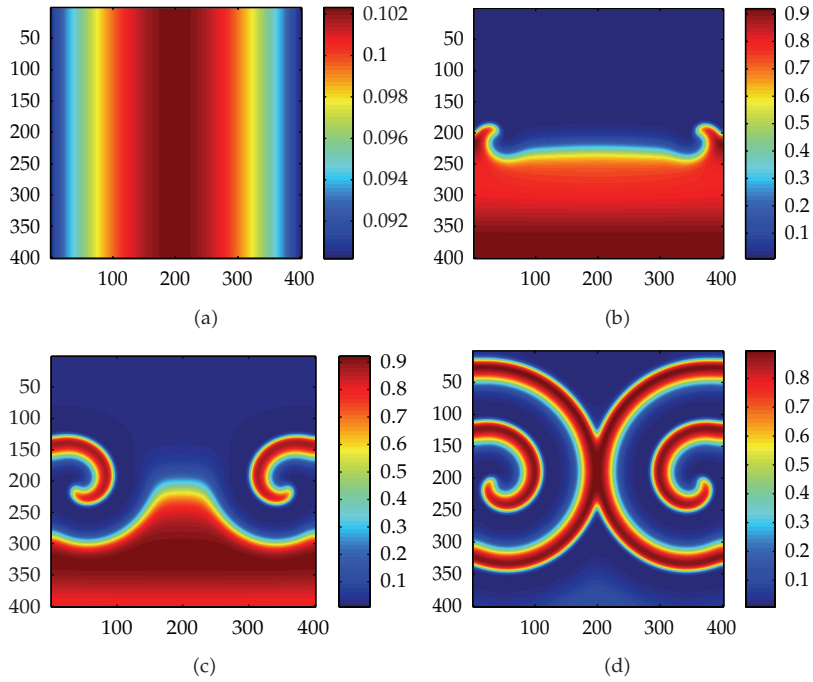

Figure 5: The process of spiral patterns of N for the parameters: $\alpha = 2.5$, $\beta = 1.3$, $\gamma = 1.1$, $d_{11} = 0.7$, $d_{12} = 0.05$, $d_{21} = 0.01$, $d_{22} = 1$. Time: (a) $t = 0$, (b) $t = 200$, (c) $t = 250$, (d) $t = 500$.

critical point (x_{cr}, y_{cr}) are (80, 200) and (320, 200), where $u(x_{cr}, y_{cr}) = u^*$, $v(x_{cr}, y_{cr}) = v^*$. The distribution (3.3) contains one point. After the spirals form (Figure 5(b)), they grow slightly for a certain time, their spatial structure becoming more distinct (Figures 5(c) and 5(d)).

4. Conclusions and Discussions

In this paper, we analyzed pattern formation of a cross-diffusion ratio-dependent predator-prey model within two-dimensional space and give the conditions of cross-diffusion-driven driven Turing instability. Then, we use numerical simulations to verify the correctness of the theoretical results and find that the model exhibits complex self-replication.

The results show that model (2.5) has rich spatiotemporal patterns (spots, stripes, holes, and spiral patterns); moreover, the existence of those patterns indicates that the cross-diffusion can induce more complex pattern formation than in the case of self-diffusion.

Compared to the paper of Lin [23], we present the condition of cross-diffusion Turing pattern, while in the case of self-diffusion the solution of the model is stable. We also show that the increasing speed of diffusion d_{12} will decrease the density of the prey. Similar, increasing speed of diffusion d_{21} will decrease density of the predator.

Therefore, we hope that the results presented here will be useful in studying the dynamic complexity of ecosystems or physical systems.

Acknowledgments

This research was supported by Fund Project of Zhejiang Provincial Education Department (Y201223449), Natural Science Foundation of Zhejiang Province (LY12A01014), and Natural Science Foundation of China (10901121).

References

[1] D. Alonso, F. Bartumeus, and J. Catalan, "Mutual interference between predators can give rise to turing spatial patterns," *Ecology*, vol. 83, no. 1, pp. 28–34, 2002.

[2] R. S. Cantrell and C. Cosner, *Spatial Ecology via Reaction-Diffusion Equations*, John Wiley & Sons, Indianapolis, Ind, USA, 2003.

[3] B. Dubey, N. Kumari, and R. K. Upadhyay, "Spatiotemporal pattern formation in a diffusive predator-prey system: an analytical approach," *Journal of Applied Mathematics and Computing*, vol. 31, no. 1-2, pp. 413–432, 2009.

[4] S. A. Levin, "The problem of pattern and scale in ecology: the Robert H. MacArthur award lecture," *Ecology*, vol. 73, no. 6, pp. 1943–1967, 1992.

[5] R. B. Hoyle, *Pattern Formation: An Introduction to Methods*, Cambridge University Press, Cambridge, UK, 2006.

[6] E. A. McGehee and E. Peacock-López, "Turing patterns in a modified Lotka-Volterra model," *Physics Letters A*, vol. 342, no. 1-2, pp. 90–98, 2005.

[7] A. Morozov and S. Petrovskii, "Excitable population dynamics, biological control failure, and spatiotemporal pattern formation in a model ecosystem," *Bulletin of Mathematical Biology*, vol. 71, no. 4, pp. 863–887, 2009.

[8] J. D. Murray, *Mathematical Biology*, Springer, New York, NY, USA, 2003.

[9] W. Wang, Q.-X. Liu, and Z. Jin, "Spatiotemporal complexity of a ratio-dependent predator-prey system," *Physical Review E*, vol. 75, no. 5, Article ID 051913, 2007.

[10] Y. Huang and O. Diekmann, "Interspecific influence on mobility and Turing instability," *Bulletin of Mathematical Biology*, vol. 65, no. 1, pp. 143–156, 2003.

[11] S. A. Levin and L. A. Segel, "Hypothesis for origin of planktonic patchiness," *Nature*, vol. 259, no. 5545, p. 659, 1976.

[12] J. D. Murray, "Discussion: turing's theory of morphogenesis—its influence on modelling biological pattern and form," *Bulletin of Mathematical Biology*, vol. 52, no. 1-2, pp. 117–152, 1990.

[13] A. M. Turing, "The chemical basis of morphogenesis," *Philosophical Transactions of the Royal Society B*, vol. 237, pp. 37–72, 1952.

[14] L. A. Segel and J. L. Jackson, "Dissipative structure: an explanation and an ecological example," *Journal of Theoretical Biology*, vol. 37, no. 3, pp. 545–559, 1972.

[15] A. Gierer and H. Meinhardt, "A theory of biological pattern formation," *Biological Cybernetics*, vol. 12, no. 1, pp. 30–39, 1972.

[16] A. Okubo and S. A. Levin, *Diffusion and Ecological Problems: Modern Perspectives*, Springer, New York, NY, USA, 2001.

[17] W. M. Wang, H. Y. Liu, Y. L. Cai, and Z. Q. Li, "Turing pattern selection in a reaction-diffusion epidemic model," *Chinese Physics B*, vol. 20, no. 7, Article ID 074702, 2011.

[18] W. Wang, Y. Lin, L. Zhang, F. Rao, and Y. Tan, "Complex patterns in a predator-prey model with self and cross-diffusion," *Communications in Nonlinear Science and Numerical Simulation*, vol. 16, no. 4, pp. 2006–2015, 2011.

[19] W. M. Wang, W. J. Wang, Y. Z. Lin, and Y. J. Tan, "Pattern selection in a predation model with self and cross diffusion," *Chinese Physics B*, vol. 20, no. 3, Article ID 034702, 2011.

[20] Y.-H. Fan and W.-T. Li, "Permanence for a delayed discrete ratio-dependent predator-prey system with Holling type functional response," *Journal of Mathematical Analysis and Applications*, vol. 299, no. 2, pp. 357–374, 2004.

[21] X. Liu and L. Huang, "Permanence and periodic solutions for a diffusive ratio-dependent predator-prey system," *Applied Mathematical Modelling*, vol. 33, no. 2, pp. 683–691, 2009.

[22] X. Zeng and Z. Liu, "Nonconstant positive steady states for a ratio-dependent predator-prey system with cross-diffusion," *Nonlinear Analysis*, vol. 11, no. 1, pp. 372–390, 2010.

[23] W. Lin, "Spatial pattern formation of a ratio-dependent predator prey model," *Chinese Physics B*, vol. 19, no. 9, Article ID 090206, 2010.
[24] V. N. Biktashev, J. Brindley, A. V. Holden, and M. A. Tsyganov, "Pursuit-evasion predator-prey waves in two spatial dimensions," *Chaos*, vol. 14, no. 4, pp. 988–994, 2004.
[25] J. B. Shukla and S. Verma, "Effects of convective and dispersive interactions on the stability of two species," *Bulletin of Mathematical Biology*, vol. 43, no. 5, pp. 593–610, 1981.
[26] E. H. Kerner, "Further considerations on the statistical mechanics of biological associations," *Bulletin of Mathematical Biophysics*, vol. 21, pp. 217–255, 1959.
[27] N. Shigesada, K. Kawasaki, and E. Teramoto, "Spatial segregation of interacting species," *Journal of Theoretical Biology*, vol. 79, no. 1, pp. 83–99, 1979.
[28] J. Chattopadhyay and P. K. Tapaswi, "Effect of cross-diffusion on pattern formation—a nonlinear analysis," *Acta Applicandae Mathematicae*, vol. 48, no. 1, pp. 1–12, 1997.
[29] B. Dubey, B. Das, and J. Hussain, "A predator-prey interaction model with self and cross-diffusion," *Ecological Modelling*, vol. 141, no. 1–3, pp. 67–76, 2001.
[30] M. Iida, M. Mimura, and H. Ninomiya, "Diffusion, cross-diffusion and competitive interaction," *Journal of Mathematical Biology*, vol. 53, no. 4, pp. 617–641, 2006.
[31] K. Kuto and Y. Yamada, "Multiple coexistence states for a prey-predator system with cross-diffusion," *Journal of Differential Equations*, vol. 197, no. 2, pp. 315–348, 2004.
[32] G. Q. Sun, Z. Jin, Q. X. Liu, and L. Li, "Pattern formation induced by cross-diffusion in a predator-prey system," *Chinese Physics B*, vol. 17, no. 11, pp. 3936–3941, 2008.
[33] V. K. Vanag and I. R. Epstein, "Cross-diffusion and pattern formation in reaction-diffusion systems," *Physical Chemistry Chemical Physics*, vol. 11, no. 6, pp. 897–912, 2009.
[34] W. Ko and K. Ryu, "On a predator-prey system with cross diffusion representing the tendency of predators in the presence of prey species," *Journal of Mathematical Analysis and Applications*, vol. 341, no. 2, pp. 1133–1142, 2008.
[35] W. Ko and K. Ryu, "On a predator-prey system with cross-diffusion representing the tendency of prey to keep away from its predators," *Applied Mathematics Letters*, vol. 21, no. 11, pp. 1177–1183, 2008.
[36] A. B. Medvinsky, S. V. Petrovskii, I. A. Tikhonova, H. Malchow, and B.-L. Li, "Spatiotemporal complexity of plankton and fish dynamics," *SIAM Review*, vol. 44, no. 3, pp. 311–370, 2002.
[37] R. K. Upadhyay, W. Wang, and N. K. Thakur, "Spatiotemporal dynamics in a spatial plankton system," *Mathematical Modelling of Natural Phenomena*, vol. 5, no. 5, pp. 102–122, 2010.